Clin. Exp. Metastasis, 1992, **10**, 403–410

A quantitative model for spontaneous bone metastasis: evidence for a mitogenic effect of bone on Walker 256 cancer cells

Paul J. Kostenuik, Gurmit Singh, Kaye L. Suyama and F. William Orr

Department of Pathology, Oncology Research Group, McMaster University, and Hamilton Regional Cancer Centre, Hamilton, Ontario, Canada

(Received 10 April 1992; accepted 22 June 1992)

A new model for the study of spontaneous bone metastasis has been developed which allows for the quantification of metastatic tumor burden and cancer cell growth rate, and which describes the progressive changes in bone morphology. Walker 256 (W256) cells or vehicle were injected into the left upper thigh muscle of male Fischer rats, which were killed 7, 10 or 14 days later. By day 7, metastases had appeared in the distal femur, in the glomeruli of the kidney, and diffusely throughout the liver and lungs. The extent of tumor burden in these organs increased over time. In the femur, 14 days of tumor burden was associated with a 53 ± 10% decrease in trabecular bone content, a 61 ± 15% increase in osteoclast surface, and a 95 ± 10% decrease in osteoblast surface, as compared with non-tumor-bearing controls. By autoradiography, metastatic tumor cells in all organs were determined to have greater growth rates than did cells in the primary tumor. However, within the femur, W256 cells located adjacent to trabecular bone surfaces had a 33 ± 7% greater growth rate than did W256 cells located >50 μm from bone surfaces ($P < 0.05$), suggesting a mitogenic effect of bone.

Keywords: bone metastasis, growth, hypercalcemia, Leydig cell tumor, osteolysis

Introduction

Metastasis is a multistep process involving a cascade of events which results in the formation of colonies of tumor cells at locations which are distant from the primary tumor. The circulatory system provides a common route for cancer cells to disseminate throughout the body. Primary human malignancies often have distinct, predictable patterns of metastasis which are independent of the first capillary bed encountered by circulating tumor cells [1]. Thus, the pattern and location of metastatic foci cannot always be explained in terms of their anatomical relationship with the primary tumor.

Address correspondence to: Dr F. W. Orr, McMaster University, Department of Pathology, 1200 Main Street West, Room 2V17B, Hamilton, Ontario, Canada L8N 3Z5.

Bone is a frequent site of metastasis for several common human malignancies, including breast, prostate, lung, and thyroid carcinomas. Bone metastasis is frequently associated with extensive osteolysis and hypercalcemia [2–4]. An explanation for the phenomenon of selective skeletal metastases may be related to the unique metabolic properties of bone. Bone metabolism involves constantly alternating phases of formation and breakdown. These processes result in the release of organic and inorganic components of bone mineral and matrix into both the bone microenvironment and the circulation. Some of these components, including collagen fragments [5] and transforming growth factor-β (TGF-β) have been shown *in vitro* to be potently mitogenic [6] and chemotactic [7] for the Walker 256 (W256) carcinosarcoma, a rat

tumor of monocytoid origin [8] which produces extensive skeletal metastases [9, 10]. Similar effects were also identified in conditioned culture media obtained from resorbing fetal rat calvaria. The ability of bone-derived conditioned media to stimulate growth and chemotaxis correlated directly with the extent of bone resorption [6, 7, 11–14]. The responses of the W256 cells to conditioned media could be largely inhibited by the addition of anti-TGF-β antibody [6, 7].

This work has suggested that bone-derived growth factors including TGF-β, released by remodeling bones, might attract tumor cells to bone and subsequently stimulate their growth rate. To investigate this hypothesis *in vivo*, we have developed a model of spontaneous bone metastases by W256 tumor cells in the rat which is amenable to the analysis of bone remodeling, and which allows for the evaluation of tumor burden and cancer cell growth response. This model has permitted us to establish the pattern of spread of tumor cells, their growth rates in primary and metastatic sites, and their effects on the structure and metabolism of bone. We argue that this model is more relevant to mechanisms of bone metastasis than other *in vivo* models which involve direct invasion of bone from contiguous intramuscular tumor [15, 16], intraosseous injection of W256 cells [17] or non-spontaneous metastasis via intra-arterial injection [10, 15, 18–20]. This is the first detailed study to describe the spontaneous hematogenous spread of W256 cells from a solid primary tumor over time, and provides quantified histologic analysis of distant metastatic target organs, including bone and soft tissues.

Materials and methods

Animals and cell lines

Female Fischer 344 rats (150–175 g) were purchased from Charles River Laboratories (St Constant, Quebec, Canada). Animals were kept under a 12-h light/dark cycle and were provided rodent chow and water *ad libitum*. The properties, maintenance, and isolation of the Walker 256 cells (Flow Laboratories) have been described previously in detail [21].

Model design

Three groups of rats ($n = 6$/group) were injected intramuscularly in the left upper thigh with 2×10^7 Walker 256 cells suspended in 0.5 ml 1 × Hanks' solution. Control animals ($n = 6$) were injected with 0.5 ml 1 × Hanks' solution without tumor cells. Animals were killed on day 7, 10 or 14. Two hours prior to death, tumor-bearing animals were injected intraperitoneally with 2 μCi of [^{3}H]thymidine (Dupont, Canada) (sp. act. 81 Ci/mmol) for the subsequent autoradiographic determination of tumor cell growth rate. The right and left femurs were removed, dissected free of soft tissue, and fixed with a solution of dimethylsulphoxide (DMSO) containing 10% formalin. Primary tumors, lungs, liver, and kidneys were also removed and fixed in 10% formalin/DMSO. After 24 h of fixation the distal third of each femur was bisected longitudinally and fixed for an additional 24 h. Undecalcified bones and primary tumor samples were then dehydrated in ethanol and impregnated with Historesin (LKB, Bromma, Sweden). Tissues were sectioned with a Sorvall JB-4A microtome (Dupont, Newtown, CT, USA), and only those sections which were essentially devoid of crush artifact were used for morphometry. A 2 μm primary tumor section and sections of bones from each animal were attached to the same slide. Several 2 μm sections of each tissue were cut. One slide was stained with 1% Toluidine Blue (pH 6.9), and used for morphometric analysis, and another was used to compare the autoradiographic labeling indices of the primary tumor and metastatic cells in bone. A 10% formalin-fixed sample of each primary tumor was processed with the sections of lung, liver, and kidney and embedded in paraffin. Three μm sections were prepared and used for autoradiographic determination of [^{3}H]thymidine incorporation.

Bone morphometry

Bone morphometry was performed on the 2 μm undecalcified, longitudinal sections of the distal third of both femurs. A Mertz graticule [22] was used to obtain measurements for bone morphometry. The area of bone proximal to the distal epiphyseal growth plate was analysed under oil immersion light microscopy (× 1000 magnification). The percentage of each microscopic field (100 fields/bone section) occupied by mineralized trabecular bone was determined by recording the presence or absence of trabecular bone at 36 point measurements (trabecular bone content). Values for tumor cell content were obtained by recording the presence or absence of W256 cells at each of 36 point measurements taken in 100 fields. The percentage of trabecular bone surface occupied by osteoblasts, osteoclasts, and W256 cells were ob-

tained by recording their presence or absence where a trabecular bone surface was intercepted by the grid of the Mertz graticule. Osteoblast surface, osteoclast surface, and W256 cell surface were calculated as the length of trabecular bone surface occupied by osteoblasts, osteoclasts, and W256 cells, respectively, divided by the total trabecular bone length, the quotient of which was multiplied by 100 [23]. All analyses were performed at distances of 100, 200, 300, 400, 500, and 600 μm from the epiphyseal growth plate, in order to control for the variation of bone morphology and metabolism with proximity to the growth plate of growing animals. For statistical comparison, measurements for all the distances from the growth plate were pooled, and the overall means were compared. Measurements of tumor burden were obtained for each organ by counting the number of tumor cells per high power field, which represented 0.0133 mm^2 of tissue.

Measurement of tumor cell growth rate

Slides of primary tumor, bone sections, and soft tissue organs were coated with NTB2 autoradiographic emulsion (Kodak, Canada). Plastic-embedded sections of primary tumor and bones were stored at 4°C for 8 weeks after exposure to radiographic emulsion, and the paraffin-embedded sections of primary tumor, lung, liver and kidney were stored similarly for 2 weeks. The different incubation periods were required due to the difference in densities of the paraffin and plastic embedding media. Slides were developed, fixed, and then stained with either 1% Toluidine Blue (pH 6.9) for the plastic-embedded tissue or hematoxylin and eosin for the paraffin-embedded tissue.

Cellular uptake of [^{3}H]thymidine was detected by the appearance of black grains on the photographic emulsion over the cells. The number of grains visible above 100 cells from each primary tumor, bone, lung, liver and kidney section were counted. Two compartments of tumor cells in bone were analysed: those tumor cells immediately adjacent to trabecular bone and those tumor cells which were located >50 μm from trabecular bone, as determined with an ocular micrometer. The number of grains required for a cell to be considered positive varied according to the degree of uptake in each animals' primary tumor cells. For each primary tumor, the mean number of grains per W256 cell plus one standard deviation was calculated and this number was used as the minimum for a primary or metastatic cell to be counted as *positive*. Non-specific [^{3}H]thymidine uptake was determined by counting grains on areas of tissue which had been exposed to emulsion but which were devoid of cells.

Statistical analysis

Values for tumor-bearing rats at each time point were compared to those of non-tumor-bearing controls using the Student's *t*-test with a 95% level of confidence. All data presented represent mean ± S.E.

Results

Bone morphometry

Since no morphometric differences were observed between the femurs ipsilateral to and contralateral to the site of tumor injection, all morphometric data presented represent observations from the contralateral femur. By day 7 after tumor injection there was histologic evidence of bone metastasis in the distal femur of all tumor-bearing animals. The proportion of area of the distal epiphyseal growth plate region occupied by tumor cells increased from 0.8 ± 0.2% at day 7 to 3.1 ± 0.2% at day 10 and to 9.6 ± 0.6% at day 14 (Figure 1a). The involvement of bone by tumor cells was associated with a decrease in area occupied by trabecular bone, from 40 ± 3% in control rats to 19 ± 3% after 14 days of tumor burden (Figure 1b). The relative distribution of cells on the surface of bone trabeculae was also altered by bone metastasis. W256 cell surface increased progressively to 11 ± 1% by day 14 (Figure 2a). Increases in osteoclast surfaces were seen at 10 days (30 ± 2% increase) and at 14 days (29 ± 4% increase) compared to non-tumor-bearing controls (Figure 2b). These increases were accompanied by dramatic decreases in osteoblast surface, which declined from 22 ± 2% in control rats to 2 ± 0.3% at day 10, and to 1 ± 0.2% at day 14 (Figure 2c). W256 cell surface increased progressively to 11 ± 1% by day 14 (Figure 2c).

Tumor burden

The number of tumor cells per mm^2 of tissue was determined morphometrically in the liver, kidney, lung and distal femur (Table 1). At day 7, there was an average of 365 ± 31 W256 cells/mm^2 in bone. The tumor burden in the liver and lung at this time point was similar, and in the kidney was significantly less (18 ± 6 cells/mm^2). Tumor burden in bone increased after day 7, to 922 ± 118 cells/mm^2 by day 14. While the liver developed an

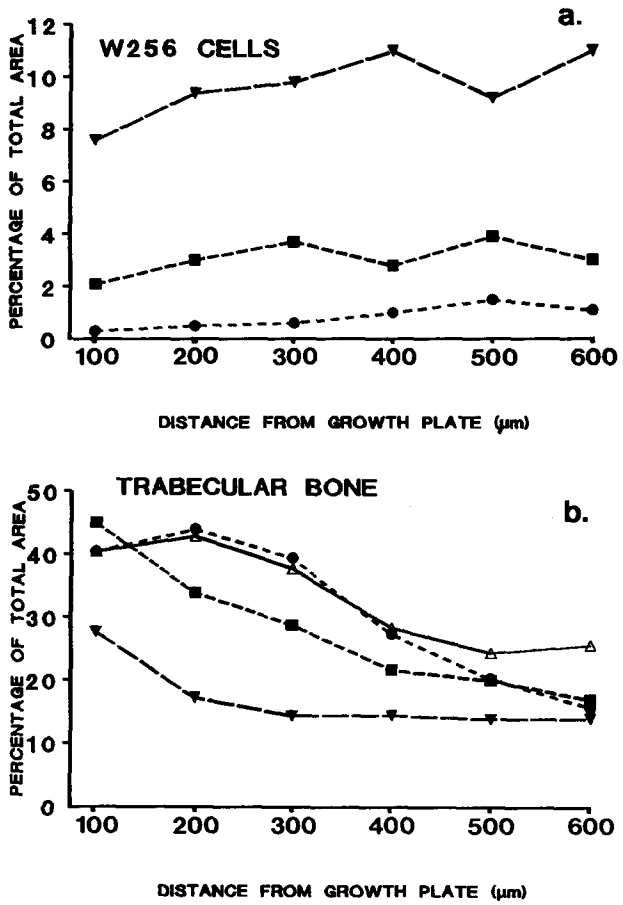

Figure 1. The percentage of total epiphyseal area occupied by (a) W256 cells and (b) trabecular bone. Rats were injected intramuscularly with 2×10^7 W256 cells, and were killed after 7 (●), 10 (■) or 14 (▼) days, and an additional group (△) was killed 14 days after vehicle injection.

equally dramatic increase in tumor burden by day 14, tumor burden in the lung and kidney increased to a lesser extent.

[^{3}H]Thymidine incorporation

The relative growth rates of metastatic tumor cells in bone, liver, lung and kidney were compared to those of cells from the primary tumor (Table 2). The relative labeling index represented the proportion of positive W256 cells in each metastatic site divided by the proportion of positive W256 cells in the primary tumor. Labeling of W256 cells in bone was 6-fold greater than in cells of the primary tumor. The labeling index of W256 cells in bone and in other soft tissue target organs was approximately the same. The relative labeling index of tumor cells adjacent to bone (6.2 ± 0.5) was significantly greater ($33 \pm 12\%$) than that of tumor

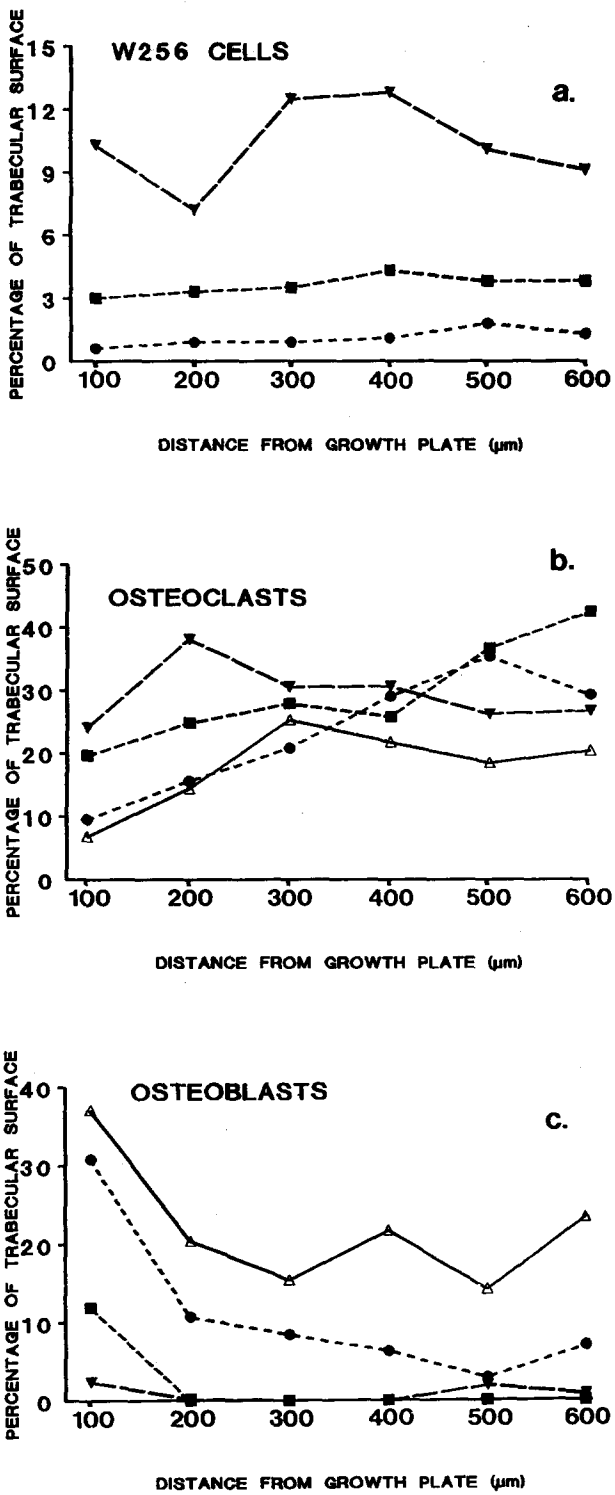

Figure 2. The percentage of total trabecular bone surface length occupied by (a) W256 cells, (b) osteoclasts, and (c) osteoblasts. Rats were injected with 2×10^{-7} W256 cells and killed after 7 (●), 10 (■) or 14 (▼) days, and an additional group (△) was killed 14 days after vehicle injection.

Table 1. W256 tumor burden in bone and in non-osseous organs. Values represent mean ± S.E.M.

	No. of W256 cells/mm² of tissue			
	7 Days	10 Days	14 Days	Overall
Bone	365 ± 31	454 ± 35	922 ± 118	580 ± 83
Liver	460 ± 95	682 ± 46[a]	1175 ± 69	780 ± 106
Kidney	18 ± 6[a]	28 ± 9[a]	34 ± 6[a]	27 ± 5[a]
Lung	433 ± 10	542 ± 75	482 ± 57[a]	485 ± 44

[a]Significantly different than bone tumor burden ($P < 0.05$).

cells located >50 μm from trabecular bone surfaces (4.8 ± 0.3, $P < 0.05$). A photograph of a typical tumor-bearing bone section prepared for autoradiography depicts this phenomenon (Figure 3).

Discussion

This study describes a quantitative model for investigating the spontaneous metastasis of tumor cells to bone. This model analyses the spontaneous hematogenous metastasis of intramuscularly-injected W256 tumor cells to bone and other organs, with detailed histomorphometry of bone and comparison of primary and metastatic tumor cell growth rate. The W256 carcinosarcoma has been well established as a tumor model which consistently invades [16, 17] and metastasizes to bone [18, 20], where it causes significant osteopenia [9, 10, 17, 18] and often hypercalcemia [9, 18, 19]. This study is the first to describe the spontaneous hematogenous spread of W256 cells from a solid primary tumor over time, and which provides detailed, quantified histologic analysis of distant metastatic target organs, including bone and soft tissues. The model represents a significant advance for the study of bone metastasis compared to other *in vivo* models which involve the invasion of bone from contiguous intramuscular tumors [15, 16], the intraosseous injection of W256 cells [17], or non-spontaneous metastasis via intraarterial injection [10, 15, 18–20]. Furthermore, several W256 models have employed non-quantitative [15, 17] and/or non-histologic methods [9, 16, 18] such as X-ray analysis [15–18] in the attempt to detect osteolysis or bone metastasis.

In the right femur, as with liver and lung, a progressive increase in tumor burden was observed over a 14-day period following the intramuscular injection of W256 cells into the left upper thigh, while colonization of the kidney was negligible at all times observed. Although tumor burden has not been previously quantified histologically in multiple organ sites, Schmidt-Gayk *et al.* [19] reported the absence of histologically evident bone metastases 8 days after intra-aortic injection of 8×10^5 W256 cells. Details of histologic processing

Table 2. Growth rates of W256 cells in various target organs relative to growth rate of primary W256 cells. Values (mean ± S.E.M.) represent the labeling index of metastatic W256 cells divided by the labeling index of primary W256 cells from each rat (see Materials and Methods for calculation of labeling index)

	Labeling indices of metastatic/primary W256 cells			
	7 Days[a]	10 Days[a]	14 Days[a]	Overall
Bone	5.8 ± 0.5	5.6 ± 0.4	7.2 ± 1.0	6.2 ± 0.5
Marrow	4.8 ± 0.1	4.3 ± 0.6	5.1 ± 0.7	4.8 ± 0.3[b]
Liver	6.8 ± 0.8	5.5 ± 0.8	6.6 ± 1.0	6.3 ± 0.3
Kidney	6.6 ± 0.8	5.5 ± 0.7	6.3 ± 0.7	6.2 ± 0.2
Lung	5.4 ± 0.4	5.7 ± 0.9	5.0 ± 0.5	5.4 ± 0.2

[a]At 7 days, 12.5 ± 0.9% of primary W256 cells were labeled, 14.3 ± 1.5% at day 10, and 12.8 ± 2.2% at day 14.
[b]Significantly less than bone labeling index ($P < 0.05$).

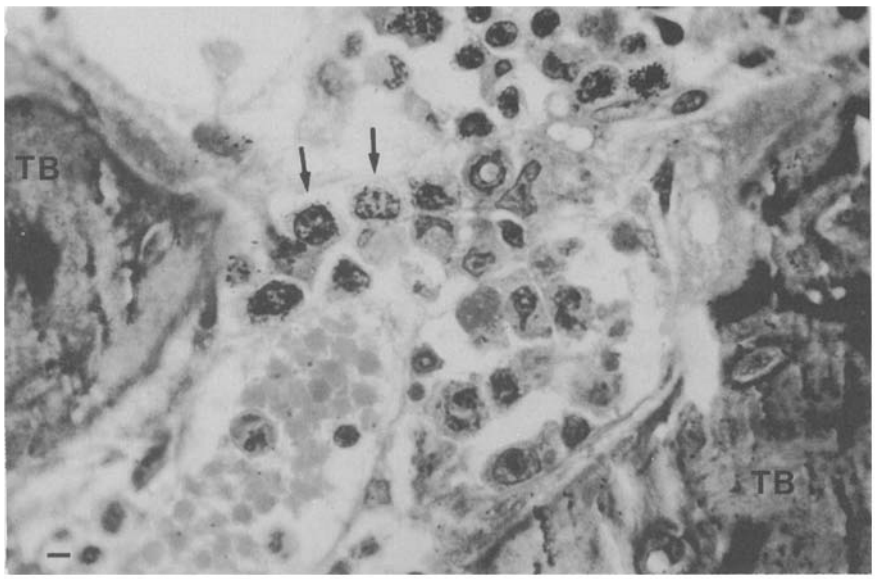

Figure 3. Autoradiographic section of a femoral epiphysis demonstrating the typical pattern of [^{3}H]thymidine uptake by W256 cells in bone. Arrows demonstrate a W256 cell adjacent to trabecular bone (TB) with extensive nuclear [^{3}H]thymidine incorporation (indicated by black grains) and a W256 cell located >50 μm from the bone surface which has less extensive [^{3}H]thymidine uptake. Bar = 10 μm.

and analysis were not provided, but lack of visible metastases may be due to the smaller number of tumor cells injected, and the shorter duration of tumor burden. At a comparable duration of tumor burden in the present study, less than 1% of the femoral epiphysis was occupied by W256 cells. W256 cell content at this site progressed to approximately 10% of total area by day 14.

In this study, occupation of bone by W256 cells was accompanied by a dramatic decrease in trabecular bone volume. This osteopenia might be explained by a 61 ± 15% increase in osteoclast surface at day 14 in tumor-bearing compared to non-tumor-bearing animals. This explanation is confounded by a significant colonization of the trabecular bone surfaces by W256 cells at day 14. Like osteoclasts, the W256 tumor has recently been shown to be of monocytoid origin and to stain intensely for acid phosphatase activity [8], which suggests that it may be capable of resorbing bone directly. This study suggests a third possible mechanism of osteopenia which may be independent of osteoclast- or tumor-induced osteolysis. The nearly complete disappearance of osteoblasts after 14 days of tumor burden could contribute to the observed decrease in trabecular bone content by preventing bone formation in the presence of unimpaired or stimulated bone resorption. While it is possible that the disappearance of osteoblasts is a secondary event in response to enhanced resorptive activity, it is more common for episodes of enhanced bone resorption to result in reactive bone formation [24], which was not observed in our tumor-bearing animals. While it is possible that poor nutrition, cachexia, or other paraneoplastic effects contributed to demineralization in tumor-bearing rats, these animals did not appear to be cachectic or to be suffering from poor nutrition until days 8–10 of tumor burden. It is likely that influences subsequent to this point would contribute minimally to the extensive osteopenia we observed in these animals.

After 14 days of tumor burden, animals did not become hypercalcemic, despite a significant loss of trabecular bone. The W256 tumor has been reported to cause hypercalcemia within the time frame of the present study [9, 17–19]. This discrepancy may be due to the different routes of tumor cell inoculation employed with previous animal models. Some models employed subcutaneous [19], intra-arterial [18], or intra-osseous [17] injection of W256 cells, which may influence the development of hypercalcemia as a function of the more direct route of administration compared to intramuscular injection.

The growth rate of metastatic tumor cells in different organs, as determined autoradiographically by [^{3}H]thymidine incorporation, was not rel-

ated to tumor burden in the corresponding organ. While the lung had a significantly greater tumor burden than did bone or liver, and while the kidney had negligible metastases, the relative growth rates of W256 cells in these organs were not different. Tumor growth rate is only one of several determinants of tumor burden, and several factors, including blood flow [25], protease activity [26], and adhesion [27], also contribute to the establishment of metastases.

All metastatic tumor cells had significantly greater growth rates compared to the primary tumors from which they originated, suggesting that the metastatic subpopulation of W256 cells may have an inherently greater growth rate than the parent population. The metastatic phenotype of the Lewis lung carcinoma has been reported to possess this property *in vitro* independent of the addition of exogenous growth factors [27]. Alternatively, organs which support metastasis may in some way stimulate the growth rate of disseminated W256 cells. The ability of organ cultures to preferentially support or stimulate the growth of the metastatic tumor cells lines which consistently colonize them is well documented [28–30], and it is possible that each target organ elaborates factors(s) which are mitogenic to circulating tumor cells. While we did not attempt to determine the cause for increased [^{3}H]thymidine uptake by metastatic tumor cells compared to primary tumor cells, it is also plausible that this observed phenomenon is related to vasculature and blood supply, which might favor the delivery of oxygen and nutrients to metastatic cells.

Within the femur, the growth rate of W256 cells in direct contact with trabecular bone was significantly greater than that of W256 cells located >50 μm from bone. The growth rate of tumor cells distant from bone was lower than that of all other metastatic tumor cells, which may indicate inhibition of these metastatic cells by a factor(s) located in the marrow. It is difficult to resolve why such inhibition would not act on tumor cells adjacent to bone, which are also bathed in marrow and in contact with marrow cells. An alternative possibility is that trabecular bone stimulates growth of the W256 cells in contact with them. This explanation would be consistent with reports that the products of resorbing bone can stimulate the chemotaxis [5, 6, 11–13] and the growth [6, 11, 14] of W256 cells. Recently, factors released from bone fibroblasts have been implicated in the accelerated growth rate of human prostate cancer cells in nude mice [31]. Similar factors released from bone cells into their microenvironment may accelerate the growth of W256 cells in their proximity.

This study provides the first *in vivo* evidence for a role of bone in the regulation of the growth rate of metastatic tumor cells, and suggests that if a factor(s) secreted by remodeling bones is involved, it is effective over a relatively short distance. The increase in resorptive bone surfaces seen in tumor-bearing animals may establish a servomechanism whereby the degradation of bone by tumor cells or tumor cell-activated osteoclasts provides a stimulus for chemotaxis and growth of metastatic cancer cells.

Acknowledgement

Supported by a grant from the Medical Research Council of Canada (MA-10409).

References

1. Nicolson GL, 1988, Organ specificity of tumor metastasis: role of preferential adhesion, invasion and growth of malignant cells at specific secondary sites. *Cancer and Metastasis Reviews*, **7**, 143–188.
2. Percival RC, Yates AJP, Gray RES, Galloway J, Rogers K, Neal FE and Kanis JA, 1985, Mechanisms of malignant hypercalcemia in carcinoma of the breast. *British Medical Journal*, **291**, 776–777.
3. Plesnicar S, 1985, The course of metastatic disease originating from carcinoma of the prostate. *Clinical and Experimental Metastasis*, **3**, 103–110.
4. Elte JWF, Bijvoet OLM, Cleton FJ, Van Oosterom AT and Sleeboom HP, 1986, Osteolytic bone metastases in breast carcinoma: pathogenesis, morbidity, and bisphosphonate treatment. *European Journal of Cancer and Clinical Oncology*, **22**, 493–500.
5. Mundy GR, Demartino S and Rowe DW, 1981, Collagen and collagen-derived fragments are chemotactic for tumor cells. *Journal of Clinical Investigation*, **68**, 1102–1105.
6. Millar-Book W, Orr FW and Singh G, 1990, *In vitro* effects of bone and platelet-derived transforming growth factor-β on the growth of Walker 256 carcinosarcoma cells. *Clinical and Experimental Metastasis*, **8**, 503–510.
7. Orr FW, Millar-Book W and Singh G, 1990, Chemotactic activity of bone and platelet-derived transforming growth factor beta for bone-metastasizing rat Walker 256 carcinosarcoma cells. *Invasion and Metastasis*, **10**, 241–252.
8. Simpkins H, Lehman JM, Mazurkiewicz JE and Davis BH, 1991, A morphological and phenotypical analysis of Walker 256 cells. *Cancer Research*, **51**, 1334–1338.

9. Minne H, Ratte F, Bellwinkel S and Ziegler R, 1975, The hypercalcemic syndrome in rats bearing the Walker carcinosarcoma 256. *Acta Endocrinologica*, **78**, 613–624.
10. Jung A, Bornand, J, Mermillod B, Edouard C and Meunier PJ, 1984, Inhibition by diphosphonates of bone resorption induced by the Walker tumor of the rat. *Cancer Research*, **44**, 3007–3011.
11. Orr FW, Varani J, Gondek MD, Ward PA and Mundy GR, 1979, Chemotactic responses of tumor cells to products of resorbing bone. *Science*, **203**, 176–179.
12. Orr FW, Varani J, Gondek MD, Ward PA and Mundy GR, 1980, Partial characterization of a bone-derived chemotactic factor for tumor cells. *American Journal of Pathology*, **99**, 43–52.
13. Magro C, Orr FW, Manishen WJ, Sivananthan K and Mokashi S, 1985, Adhesion, chemotaxis, and aggregation of Walker carcinosarcoma cells in response to products of resorbing bone. *Journal of the National Cancer Institute*, **74**, 829–834.
14. Manishen WJ, Sivananthan K and Orr FW, 1986, Resorbing bone stimulates tumor cell growth. *American Journal of Pathology*, **123**, 39–45.
15. Guaitani A, Polentarutti N, Filippeschi S, Marmonti L, Corti F, Italia C, Coccioli G, Donell MG, Mantovani A and Garattini S, 1985, Effects of disodium etidronate in murine tumor models. *European Journal of Cancer and Clinical Oncology*, **20**, 685–693.
16. Bassani D, Sabatini M, Scanziani E, De Francesco L, Coccioli G, Guaitani A and Bartosek I, 1990, Bone invasion by Walker 256 carcinoma, line A in young and adult rats: effects of etidronate. *Oncology*, **47**, 160–165.
17. Krempien B, Wingen F, Eichmann T, Muller M and Schmahl D, 1988, Protective effects of a prophylactic treatment with the bisphosphonate 3-amino-1-hydroxypropylidene-1,1-bisphosphonic acid on the development of tumor osteopathies in the rat: experimental studies with the Walker carcinosarcoma 256. *Oncology*, **45**, 41–46.
18. Powles TJ, Clark SA, Easty DM, Easty GC and Neville AM, 1973, The inhibition by aspirin and indomethacin of osteolytic tumour deposits and hypercalcemia in rats with Walker tumor, and its possible application to human breast cancer. *British Journal of Cancer*, **28**, 316–321.
19. Schmidt-Gayk H, Lohrke H, Fishkal A, Goerttler K and Hofmann F, 1979, Urinary cyclic AMP and bone histology in Walker carcinosarcoma: evidence of parathyroid hormone-like activity. *European Journal of Cancer*, **15**, 1211–1218.
20. Krempien B, 1984, The Walker carcinosarcoma 256 as an experimental model of bone metastases: influence of local and metabolic factors on incidence and pattern of metastases. *Calcified Tissue International*, **36**, S26.
21. Rayner DC, Orr FW and Shiu RPC, 1985, Binding of formyl peptides of Walker 256 carcinosarcoma cells and the chemotactic response of these cells. *Cancer Research*, **45**, 2288–2293.
22. Schenk RK. Principles of bone morphometry. In: Jaworski ZFG, ed. *Proceedings of the First Workshop on Bone Morphometry*. Ottawa: University of Ottawa Press, 1976.
23. Revell PA. Quantitative methods in bone biopsy examination. In: Revell PA, ed. *Pathology of Bone*. New York, NY: Springer Verlag, 1986.
24. Nemoto R, 1991, New bone formation and cancer implants: relationship to tumor proliferative activity. *British Journal of Cancer*, **63**, 348–350.
25. Weiss L, Haydock K, Pickren JW and Lane WW, 1980, Organ vascularity and metastatic frequency. *American Journal of Pathology*, **101**, 101–114.
26. Turpeenniemi-Hujanen T, Thorgeirsson UP, Hart IR, Grant SS and Liotta LA, 1985, Expression of collagenase IV (basement membrane collagenase) activity in murine tumor cell hybrids that differ in metastatic potential. *Journal of the National Cancer Institute*, **75**, 99–103.
27. Perrotti D, Cimino L, Falcioni R, Tibursi G, Gentileschi MP and Sacchi A, 1990, Metastatic phenotype: growth factor dependence and integrin expression. *Anticancer Research*, **10**, 1587–1598.
28. Nicolson GL and Dulski KM, 1986, Organ specificity of metastatic tumor colonization is related to organ-selective growth properties of malignant cells. *International Journal of Cancer*, **38**, 289–294.
29. Naito S, Giavazzi R and Fidler IJ, 1987, Correlation between the *in vitro* interaction of tumor cells with an organ environment and metastatic behaviour *in vivo*. *Invasion and Metastasis*, **7**, 16–29.
30. Sargent NSE, Oestreicher M, Haidvogl H, Madnick HM and Burger MM, 1988, Growth regulation of cancer metastases by their host organ. *Proceedings of the National Academy of Sciences, U.S.A.*, **85**, 7251–7255.
31. Gleave M, Hsieh JT, Gao C, Von Eschenbach AC and Chung LWK, 1991, Acceleration of human prostate cancer growth *in vivo* by factors produced by prostate and bone fibroblasts. *Cancer Research*, **51**, 3753–3761.